American Journal of Pathology, Vol. 168, No. 5, May 2006

DOI: 10.2353/ajpath.2006.050533

Vascular Biology, Atherosclerosis and Endothelium Biology

Expression of Protein Kinase CK2 in Astroglial Cells of Normal and Neovascularized Retina

Andrei A. Kramerov,* Mehrnoosh Saghizadeh,* Hao Pan,† Andrea Kabosova,* Mathias Montenarh,‡ Khalil Ahmed,§ John S. Penn,¶ Candy K. Chan,‖ David R. Hinton,‖ Maria B. Grant,† and Alexander V. Ljubimov*

From the Ophthalmology Research Laboratories, Cedars-Sinai Medical Center, University of California at Los Angeles School of Medicine, Los Angeles, California; the Department of Pharmacology,† University of Florida, Gainesville, Florida; the Minneapolis Veterans Affairs Medical Center,§ University of Minnesota, Minneapolis, Minnesota; the Department of Ophthalmology and Visual Sciences,¶ Vanderbilt University School of Medicine, Nashville, Tennessee; the Departments of Pathology and Ophthalmology,‖ University of Southern California, Los Angeles, California; and Medizinische Biochemie und Molekularbiologie,‡ Universität des Saarlandes, Homburg, Germany*

We previously documented protein kinase CK2 involvement in retinal neovascularization. Here we describe retinal CK2 expression and combined effects of CK2 inhibitors with the somatostatin analog octreotide in a mouse model of oxygen-induced retinopathy (OIR). CK2 expression in human and rodent retinas with and without retinopathy and in astrocytic and endothelial cultures was examined by immunohistochemistry, Western blotting, and reverse transcriptase-polymerase chain reaction. A combination of CK2 inhibitors, emodin or 4,5,6,7-tetrabromobenzotriazole, with octreotide was injected intraperitoneally from postnatal (P) day P11 to P17 to block mouse OIR. All CK2 subunits (α, α', β) were expressed in retina, and a novel CK2α splice variant was detected by reverse transcriptase-polymerase chain reaction. CK2 antibodies primarily reacted with retinal astrocytes, and staining was increased around new intraretinal vessels in mouse OIR and rat retinopathy of prematurity, whereas preretinal vessels were negative. Cultured astrocytes showed increased perinuclear CK2 staining compared to endothelial cells. In the OIR model, CK2 mRNA expression increased modestly on P13 but not on P17. Octreotide combined with emodin or 4,5,6,7-tetrabromobenzotriazole blocked mouse retinal neovascularization more efficiently than either compound alone. Based on its retinal localization, CK2 may be considered a new immunohistochemical astrocytic marker, and combination of CK2 inhibitors and octreotide may be a promising future treatment for proliferative retinopathies. ***(Am J Pathol 2006, 168:1722–1736; DOI: 10.2353/ajpath.2006.050533)***

Neovascularization, an important physiological process during retinal development, is a combination of vasculogenesis and angiogenesis.[1,2] The superficial retinal vessels grow radially from the optic nerve by vasculogenesis, where endothelial progenitor cells and hemangioblasts differentiate to form blood vessels. Deep vessels evolve by angiogenesis in which sprouting from superficial retinal vessels occurs, causing penetration of new blood vessels into the retina. In both processes, astrocytes migrating from the optic nerve to the retina play a guiding role for sprouting capillaries.[3]

Retinal neovascularization is usually considered to be the result of proliferation of endothelial cells from the existing blood vessels by angiogenesis. However, circulating adult hematopoietic stem cells may also contribute to this process by differentiating into endothelial cells.[4] It is still unclear what fraction of endothelial cells derives from hematopoietic stem cells during retinal angiogenesis. The identity of growth factors and cytokines that

Supported by the Skirball Program in Molecular Ophthalmology; seed grants from the Department of Surgery, Cedars-Sinai Medical Center; and the National Institutes of Health (grant 2R01 EY7709).

Accepted for publication January 17, 2006.

The cDNA sequence of CK2α transcript variant 3 reported in this paper was deposited to GenBank on August 26, 2004 under accession number AY735339.

Presented in part at the annual meeting of the Association for Research in Vision and Ophthalmology, Fort Lauderdale, FL, April 2004 and May 2005; at the 4th International Conference on Protein Kinase CK2, London, Canada, August 2004; and at the Symposium on Retinal and Choroidal Angiogenesis, Nashville, TN, October 2004.

Address reprint requests to Andrei A. Kramerov, Ph.D., Ophthalmology Research Laboratories, Burns and Allen Research Institute, Cedars-Sinai Medical Center, 8700 Beverly Blvd., Davis-2025, Los Angeles, CA 90048. E-mail kramerova@cshs.org.

recruit bone marrow-derived precursors into circulation for participating in angiogenesis is not fully determined although some factors have been recently identified.[5] Also, adult mouse nonhematopoietic stem cells when injected into vitreous of neonatal eyes co-localize with retinal astrocytes that serve as a network for retinal angiogenesis.[6]

The initial stimulus for retinal neovascularization is thought to be hypoxia or ischemia that causes increases in the expression of growth factors, integrins, and proteinases resulting in the formation of new vessels. The first reaction to hypoxia is stimulation of hypoxia-inducible factor-1, which up-regulates angiogenic factors such as vascular endothelial growth factor (VEGF-A), fibroblast growth factor-2, insulin-like growth factor-I, hepatocyte growth factor, and platelet-derived growth factor.[7–9] The induction of angiogenesis depends on equilibrium between angiogenic factors and angiogenesis inhibitors including angiostatin, pigment epithelium-derived factor (PEDF), and thrombospondin-1.[9–11] Such a balance may become distorted in certain conditions leading to pathological retinal neovascularization, as seen in proliferative diabetic retinopathy (DR).

DR is the most severe ocular complication of diabetes and a major cause of blindness worldwide.[12,13] Hyperglycemia-induced advanced glycation end products[14] contribute to retinal hypoxia in diabetes, leading to early pericyte dropout and capillary closure. As the disease progresses, the resulting ischemia elicits compensatory retinal neovascularization triggered by angiogenic growth factors, notably VEGF, produced by retinal neuroglial cells, astrocytes, and Müller cells.[14,15] Animal oxygen-induced proliferative retinopathy (OIR), although developing on a nondiabetic background, proved to be a useful model in exploring roles of specific growth factors in angiogenesis[16,17] and the significance of altered cell interactions in DR pathogenesis.

Astrocytes and endothelial cells are believed to be interdependent cell populations,[2] but cellular mechanisms involved in the recruitment and differentiation of astrocyte precursor cells (spindle cells) in angiogenesis remain poorly understood. A captivating possibility is a cross talk between astrocytes and endothelial cells. The ability of astrocytes to secrete VEGF and promote retinal angiogenesis is well established.[18–20] Conversely, endothelial cell-derived leukemia inhibitory factor[21] and platelet-derived growth factor[22] can induce retinal astrocyte differentiation *in vitro*.

Studies of protein kinases in astrocyte-endothelial cell interactions may lead to establishing signaling pathways involved in retinal angiogenesis and to developing approaches for anti-angiogenic therapy. Protein kinase CK2 (formerly casein kinase 2) is a ubiquitous serine/threonine protein kinase that phosphorylates more than 300 substrates and is involved in a wide variety of biological processes, including cell proliferation, differentiation, apoptosis, and tumor development.[23–26] Our previous data have shown that CK2 inhibitors potently blocked adhesion, migration, and capillary-like tube formation by cultured retinal endothelial cells, as well as retinal neovascularization in a mouse model of OIR.[27] These data implicate CK2 in retinal angiogenesis and pathogenesis of diabetic and other proliferative retinal microangiopathies. Thus, it was of interest to examine the expression of CK2 in retinal cells. To this end, we studied CK2 localization in human retinal cells by immunohistochemistry using specific antibodies to CK2 subunits. These antibodies reacted with astrocytes of the human and rodent retinas. We also determined CK2 expression in mouse OIR and in rat retinopathy of prematurity (ROP). Finally, a combined action of CK2 inhibitors with somatostatin analogs that may inhibit different angiogenic signaling pathways was studied in the OIR model.

Materials and Methods

Immunohistochemistry

Postmortem human eyes were obtained from National Disease Research Interchange (Philadelphia, PA) within 24 hours after death. Isolated human retinal samples as well as whole human, mouse, and rat eyes were embedded in O.C.T. compound (Sakura Finetek U.S.A., Inc., Torrance, CA). Frozen sections (6 μm) were cut on a Leica CM1850 cryostat (McBain Instruments, Chatsworth, CA). Before immunofluorescent staining, sections were fixed for 5 minutes at room temperature in 3% *p*-formaldehyde in phosphate-buffered saline (PBS). Stained sections were mounted in Immuno-Fluoro mounting medium (ICN Immunobiologicals, Lisle, IL). The pictures were taken with MagnaFire digital camera (Optronics, Goleta, CA) attached to a BX40 Olympus microscope (Olympus USA, Melville, NY) and were combined using MagnaFire 2.1 software.

Specific antibodies were applied for 1 to 4 hours incubation at 20°C at the following dilutions: 1:100 mouse anti-human CK2α/α' (clone 1AD9; Santa Cruz Biotechnology, Santa Cruz, CA), 1:50 mouse anti-human CK2α/α' (clone D8E),[28] 1:50 rabbit anti-human CK2α (H-286, Santa Cruz Biotechnology), 1:200 rabbit anti-human CK2α, anti-CK2α', and anti-CK2β antibodies.[29] All tested anti-CK2 antibodies are listed in Table 1. Other antibodies included goat anti-mouse vimentin (ICN Biomedicals, Aurora, OH), goat anti-human glial fibrillary acidic protein (GFAP, Santa Cruz Biotechnology), mouse anti-pig GFAP (clone GA5; Sigma Chemical Co., St. Louis, MO), rabbit anti-human GFAP (Sigma), mouse anti-human/rat laminin γ1 chain (clone 2E8;[30] a gift from Dr. E. Engvall, the Burnham Institute, La Jolla, CA), rat anti-human/mouse perlecan (clone C11L1),[31] mouse anti-α-smooth muscle actin (clone 1A4, Sigma), rabbit anti-chicken desmin with broad interspecies cross-reactivity (Sigma), and affinity-purified rabbit anti-mouse/rat laminin (A.V. Ljubimov, unpublished). The latter three antibodies were used to visualize blood vessels in mouse and rat retinas. Immunofluorescence staining was performed as described,[31] with cross-species adsorbed secondary antibodies from Chemicon International (Temecula, CA).

In some experiments, the activity of anti-human CK2α/α' 1AD9 monoclonal antibody (mAb) was neutral-

Table 1. Antibodies to CK2 Subunits Used in This Study

Antigen	Antibody and name	Western blot	Immunostaining	Source
CK2α purified	Mouse mAb 1AD9*	Negative	Human	Santa Cruz, Calbiochem
CK2 purified	Mouse mAb D8E*	Not tested	Human cultures	Reference 28
CK2α peptide	Rabbit pAb	Not tested	Nonspecific	Calbiochem
CK2α peptide	Rabbit pAb	Positive	Human	Reference 29
CK2α peptide	Goat pAb C-18	Positive	Negative	Santa Cruz
CK2α peptide	Goat pAb N-18	Not tested	Negative	Santa Cruz
CK2α peptide	Rabbit pAb	Not tested	Negative	US Biological
CK2α peptide	Rabbit pAb	Not tested	Negative	Bethyl Laboratories
CK2α/α' peptide	Rabbit pAb H-286	Positive	Human, mouse, rat	Santa Cruz
CK2α/α' rec. N-terminal third	Mouse mAb 31	Positive	Negative	BD Transduction
CK2α' peptide	Rabbit pAb	Not tested	Human	Reference 29
CK2α' peptide	Goat pAb C-20	Not tested	Negative	Santa Cruz
CK2α' peptide	Rabbit pAb	Not tested	Negative	Bethyl Laboratories
CK2β rec.	Mouse mAb 51	Positive	Negative	BD Transduction
CK2β rec.	Rabbit pAb FL-215	Negative	Negative	Santa Cruz
CK2β rec.	Mouse mAb 6D5	Not tested	Negative	Calbiochem
CK2β peptide	Rabbit pAb	Positive	Human	Reference 29
CK2β peptide	Goat pAb C-19	Not tested	Negative	Santa Cruz

*Antibody recognizes both α and α' subunits; rec., recombinant protein; mAb, monoclonal antibody; pAb, polyclonal antibody.

ized by a corresponding blocking peptide AMEHPYFYT[32] synthesized by Invitrogen (Carlsbad, CA). The 1:50 dilution of antibody was incubated with 2 to 20 μg/ml peptide for 4 hours on a rotating stand at room temperature. After high-speed centrifugation, the supernatant was further used in immunohistochemistry.

Human optic nerve head astrocytes were isolated as described previously[33] and propagated in Dulbecco's modified Eagle's medium/F12 medium with 10% fetal bovine serum. Human brain astrocytes (NHA, Cambrex, East Rutherford, NJ; or HAST040, Clonexpress, Inc., Gaithersburg, MD) and untransformed human brain microvascular endothelial cells obtained from Dr. Ken Samoto (Kyushu University, Fukuoka, Japan) were cultured in Dulbecco's modified Eagle's medium with 10% fetal bovine serum. For immunofluorescence staining, cells were cultured on glass coverslips covered with 2% bovine skin gelatin, fixed in 3% *p*-formaldehyde in PBS for 5 minutes, permeabilized in 0.05% Triton X-100 in PBS for 15 minutes, and blocked by incubating 30 minutes in 5% normal goat serum before application of primary D8E mAb.

Isolation of Total RNA

For standard reverse transcriptase-polymerase chain reaction (RT-PCR), RNA was isolated from normal human retinas with Trizol reagent (Invitrogen) and stored at −80°C. To achieve higher purity, RNA was treated with NucleoSpin RNA and virus purification kit (BD Biosciences, Palo Alto, CA) per the manufacturer's instructions. RNA quality and yield was assessed with the Agilent 2100 bioanalyzer system (Agilent Technologies, Palo Alto, CA) and with Ultrospec 3100 pro spectrophotometer (Amersham Biosciences, Piscataway, NJ).

RT-PCR and Cloning

First-strand cDNA was synthesized using TaqMan reverse transcription reagents (Applied Biosystems, Foster City, CA) using oligo (dT) primers as described above. PCR was performed using Advantage 2 polymerase mix (BD Biosciences), 40 mmol/L Tricine-KOH (pH 9.2), 15 mmol/L KOAC, 3.5 mmol/L Mg $(OAc)_2$, 3.75 μg/ml bovine serum albumin, 0.2 mmol/L dNTP, 0.2 μmol/L PCR primers. Primers used for these studies (Table 2) were designed using Primer 3 Internet software (*http://frodo.wi.mit.edu/cgi-bin/primer3/primer3_www.cgi*) based on gene sequences from GenBank. All oligonucleotide primers for quantitative PCR were synthesized by Invitrogen. The cDNA was amplified using the following program profile: one cycle at 95°C for 2 minutes; 40 cycles at 95°C for 30 seconds, 60°C for 30 seconds, 72°C for 1 minute; followed by one cycle at 72°C for 10 minutes. Routine controls to check for possible DNA contamination included PCR amplification without the reverse transcription step and water control and were always negative. To reveal different splice variants of CK2α mRNA, forward consensus primer from exon 1 was used in combination with consensus reverse primer from exon 4 in a PCR reaction on 40 ng of cDNA. The resulting PCR products were purified using PCR gel extraction kit (Qiagen, Chatsworth, CA), and cloned using the Topo cloning kit (Invitrogen) as described by the manufacturer. Vector primers M13F and M13R were used to obtain the sequences of the cDNA clones using DYEnamic ET terminator kit (Amersham Biosciences) in an Applied Biosystems ABI Prism 3100 genetic analyzer.

Quantitative Real-Time RT-PCR (QPCR)

This was done using RNA isolated from mouse retinas. C57BL/6J mice were subjected to the OIR regimen and retinas were isolated on day 13, 24 hours after removing animals from hypoxic chamber, and on day 17 when there is maximum retinal neovascularization. Ten retinas per each data point (five normoxic control mice, days 13 and 17; and five OIR mice, days 13 and 17) were pooled and immediately frozen in RNAlater (Ambion, Austin, TX). The TRI reagent in conjunction with bromochloropropane

Table 2. RT-PCR Primer Sequences

Gene	Forward primer	Reverse primer	Product size (bp)
CK2α 3′-end; nonspliced area	5′-CTTCTCAGGGGAGGCAGGA-3′	5′-CACACTTCCACAAGAGCCACT-3′	151
CK2α′ 3′-end	5′-CACTTTTCCATAAGCAGAACAAGA-3′	5′-TACATTCGGAAGTGAGGTTTGATA-3′	163
CK2β 3′-end	5′-AAAAGTACCAGCAAGGAGACTTTG-3′	5′-GTGTCTTGATGACTTGGGTGTGTA-3′	158
CK2α exons 2 to 3; variant 1	5′-GTAAATCATGCAGCGTGGAA-3′	5′-TGTAAACTCTGGCCCTGCTT-3′	225
CK2α exons 1/3 to 3; variant 2	5′-CCACCACAGTTTGAAGAAAAC-3′	5′-TTCCACCACATGTGACTCGT-3′	214
CK2α exons 1 to 1/4; variant 3	5′-CTCCTGGTAGGAGGGGGTTT-3′	5′-TCTTGATTTCCCCATTCCAC-3′	191
CK2α exons 1 to 4; all variants have different sizes	5′-CCGCCATATTGTCTGTGTGA-3′	5′-TGATGTTGGGACCTCCTCTC-3′	572 (1), 455 (2), 245 (3)
β_2-Microglobulin	5′-ATAATTCTACTTTGAGTGCTGTCTCCAT-3′	5′-TCCTAGAGCTACCTGTGGAGCAA-3′	71
β_2-Microglobulin	5′-CTCGCGCTACTCTCTCTTTCTG-3′	5′-GCTTACATGTCTCGATCCCACTT-3′	335
CK2α/A1 mouse*	5′-GACCAGGCTCGAATGAGTTC-3′	5′-ATCGAGGAGAGGGTGGACTT-3′	281
CK2α′/A2 mouse*	5′-TGACCAGCTTGTTCGAATTG-3′	5′-GGCGGTCAATCTCTGTTGAT-3′	229
CK2β/B mouse*	5′-ATCGAACAGGCAGCTGAGAT-3′	5′-GTGGTGGTGTCTGGAGGACT-3′	246
β-Actin mouse	5′-CCTAAGGCCAACCGTGAAAAG-3′	5′-ACCGCTCGTTGCCAATAGTGA-3′	430

*Nomenclature of mouse CK2 subunits is included after a slash.

for phase separation (Molecular Research Center, Inc., Cincinnati, OH) was used to isolate total RNA and protein according to the manufacturer's instructions.

QPCR was conducted as described[34] with some modifications. Briefly, total RNA (2 μg in 20-μl reaction) was treated with TURBO DNA-free (Ambion) to remove possible genomic DNA contamination. Five μl (0.5 μg) of RNA was then reverse-transcribed into first-strand cDNA using the TaqMan reverse transcription (RT) reagents (Applied Biosystems) and oligo (dT) primers in a total volume of 25 μl. Reactions were cycled on a PTC-200 Peltier thermal cycler (MJ Research, Waltham, MA) as follows: 25°C for 10 minutes, 45°C for 45 minutes, followed by inactivation at 95°C for 5 minutes. Primers for selected genes were designed using Primer 3 Internet software (Table 2). The selected primers had melting temperatures of 59°C or 60°C and not more than two G-C pairs in the final 5-bp of the 3′-end. All QPCR primers (Table 2) were synthesized by Invitrogen and confirmed to amplify the predicted products by testing under QPCR conditions.

QPCR was performed in 25 μl of total reaction volume with 1 μl of cDNA (25 ng), 12.5 μl 2 $\times$ SYBR Green master mix (Stratagene, La Jolla, CA), and 200 nmol of sense and anti-sense primers. The reactions were performed in MicroAmp optical 96-well strips with optical caps (Applied Biosystems) using the MX3000P quantitative PCR system (Stratagene). The same thermal profile conditions were used for all primer sets. The reaction conditions were as follows: 95°C for 10 minutes, and then 40 cycles of 95°C for 30 seconds, 60°C for 1 minute, and 72°C for 30 seconds. This was followed by one cycle, 95°C for 1 minute, 55°C for 30 seconds, and 95°C for 30 seconds, to monitor the dissociation curves of PCR reactions. Signals from each sample were normalized to values obtained for a housekeeping gene, β-actin, which was assayed simultaneously with experimental samples. Serial 10-fold dilutions ranging from 0.05 to 100 ng of the control retinal cDNA were included in duplicate within each run as a standard for each target gene as well as for β-actin, and relative quantification by standard curve for each gene was analyzed. In some experiments, a comparative threshold cycle (Ct) method ($\Delta\Delta$Ct) was used to calculate the relative gene expression (fold change) between test and reference sample for genes whose primers passed an efficiency test[34] with similar results.

Controls without the RT step or without template were included for each primer pair to check for any contaminants. As another quality control measure, melting (dissociation) curves of PCR reactions were monitored to ensure that there was only a single PCR product and no primer dimers. Further testing by agarose gel electrophoresis confirmed that there was only one PCR product of the expected size.

Western Blot Analysis

Retinal extracts were obtained after homogenization of the frozen retinal samples in RIPA buffer containing the protease inhibitors cocktail (1:100, Sigma) followed by sonicating homogenates for 1 minute. After clearing the homogenate by centrifugation at 14,000 $\times$ *g* for 5 minutes at 4°C, an equal volume of 2$\times$ Laemmli's sample buffer with 10% 2-mercapthoethanol was added, and the samples were subjected to 10% polyacrylamide gel electrophoresis after incubation for 5 minutes at 100°C. Cultured cells detached from dishes were pelleted and directly put into sample buffer. Western blot analysis was performed according to the manufacturer's specifications (Invitrogen). SeeBlue Plus 2 (Invitrogen) was used as molecular mass marker, and purified CK2 holoenzyme (catalog no. 218701; Calbiochem, La Jolla, CA) as marker for CK2 subunits. Anti-CK2 subunit-specific antibodies[29] were used at 1:200 to 1:500 dilution, followed by alkaline phosphatase-conjugated secondary antibodies (Chemicon International) diluted 1:10,000. The reaction was developed using 0.2 mg/ml 5-bromo-4-chloro-3-indolyl phosphate and 0.3 mg/ml nitroblue tetrazolium in 0.1 mol/L Tris-HCl and 5 mmol/L $MgCl_2$ at pH 9.5 (Sigma).

Animal Models of Retinopathy

The rat ROP model is described in detail elsewhere.[35,36] Briefly, timed-pregnant, multiparous Sprague Dawley rats were delivered to the laboratory at ~18 days gestation. Within 4 hours after birth, litters and their mothers were placed in infant Isolette incubators, and the environment within the incubators was adjusted to 50% oxygen using the Oxycycler system (Reming Bioinstruments, Redfield, NJ). After 24 hours, the oxygen concentration was rapidly reduced to 10%, where it remained for 24 hours. The oxygen continued to cycle between 50% and 10% every 24 hours for 14 days. The animals were then removed from the incubator and kept at room air (21% oxygen) until sacrifice on day 6 after exposure (postnatal day 20).

Proliferative OIR was induced in heterozygous C57BL/6J or 129S3/SvIM neonatal mice (The Jackson Laboratory, Bar Harbor, ME) by a standard protocol.[27,37] Briefly, 7-day-old mouse pups were kept for 5 days in hyperoxia (75% oxygen), which stopped retinal vascular development. Then, they were brought to room air with 25% oxygen for 5 days, and retinas became hypoxic and responded with transient neovascularization peaking at postnatal (P) day P17. CK2 inhibitors, emodin (Sigma) or 4,5,6,7-tetrabromobenzotriazole (TBB, Calbiochem), were injected intraperitoneally into mice starting at days P11 through P17 twice daily at doses of 30 mg/kg/day in Tween-80–PEG 400 mixture.[27] Somatostatin analog, octreotide (Novartis International AG, Basel, Switzerland), was injected intraperitoneally into mice at 1 or 5 mg/kg/day in PBS. Control animals were injected with combined vehicle, Tween-80–PEG 400 mixture in PBS. In a few experiments, a somatostatin peptidomimetic, SCR-011 (RFEpharma, Gainesville, FL), was used at the same dose as octreotide with similar effect. Preliminary data showed that SCR-011 was very similar to octreotide in the extent of inhibition of preretinal neovascularization in the mouse OIR model.[38]

At the end of treatment, control and treated animals were euthanized by intraperitoneal injection with tribromoethanol (0.1 ml/g body weight). This method is consistent with the recommendations of the Panel on Euthanasia of the American Veterinary Association and was selected for its rapid action and lack of effect on tissue (especially vascular) ultrastructure. Animals were perfused through the left ventricle with 4% *p*-formaldehyde in 0.1 mol/L phosphate buffer, pH 7.4, with 50 mg/ml of 2×10^3 kd fluorescein-dextran (Sigma). One eye from each animal was used for retinal flat mounts and fluorescence photography. Fellow eyes from all mice were embedded in paraffin, and serial 6-μm sections of whole eyes were cut sagittally through the cornea parallel to the optic nerve. The mean number of preretinal nuclei per eye was counted as a measure of neovascularization on 10 sections after hematoxylin and eosin staining. In some experiments, eyes were enucleated after treatments, snap-frozen, and embedded in OCT for subsequent cryosectioning and immunofluorescence analysis. All animal procedures were conducted in strict accordance to current approved Institutional Animal Care and Use Committee protocols.

Statistical Analysis

Numbers of preretinal cell nuclei as a measure of neovascularization were compared among different groups of mice using analysis of variance (InStat software program; GraphPad Software, San Diego, CA). $P < 0.05$ was considered significant.

Results

Immunohistochemical Detection of CK2 Subunits in Retinal Astrocytes

A panel of specific antibodies to human CK2 was used to study its expression in the human retina at the protein level. Of the few antibodies to CK2 with positive immunoreactivity on frozen human retinal sections, the strongest signal was obtained with 1AD9 mAb that recognizes both α and α' subunits. It exclusively stained cell processes in the inner retina and showed complete co-distribution with the antibody to GFAP, a marker of astrocytes (Figure 1, top row). In normal retinas, the immunostaining with 1AD9 mAb and anti-GFAP was confined to tangential processes running in the main domain of astrocyte location—nerve fiber layer of the inner retina, often in close association with blood vessels (Figure 1, asterisks). At the same time, the antibody to vimentin, a Müller glial cell marker, revealed lack of co-distribution with the anti-CK2 antibody in double-label experiments (Figure 1, second row). Astrocytic processes positive for CK2 were tightly wrapped around blood vessels, whereas vimentin-positive Müller cell processes were located at a greater distance from vessel walls (Figure 1, third row). In retinas from patients with DR, GFAP was also seen in Müller cell processes (Figure 1, bottom row) in accordance with previous data on injured and diabetic retinas.[39–41] However, CK2 staining in DR retinas remained confined to astrocytes in the nerve fiber layer (Figure 1, bottom row). The specificity of the immunohistochemical reaction was tested by preincubation of the anti-CK2 1AD9 mAb with a peptide comprising its epitope[32] throughout a wide range of peptide to antibody molar ratios. A progressive loss of immunoreactivity was observed starting at 1:1 peptide:antibody molar ratio and reached maximum at 10:1 ratio (Figure 2, top row). A polyclonal antibody (pAb) H-286 with similar subunit specificity showed complete co-distribution with both 1AD9 (Figure 2, bottom row) and anti-GFAP (not shown). Thus, 1AD9 and H-286 antibodies recognized both catalytic subunits of CK2 primarily in the astrocytes.

To elucidate the subunit composition of CK2 in retinal astrocytes, we used rabbit pAbs to subunit-specific peptides of human CK2 reported to immunolabel cultured human cells.[29] These antibodies revealed the expression of all three subunits in retinal astrocytes at similar levels (Figure 3); the staining co-distributed with 1AD9 reactivity. Therefore, CK2 expressed in retinal astrocytes is composed of α, α', and β subunits. To corroborate immunohistochemical data, Western blot analysis of human retinal extracts was performed using

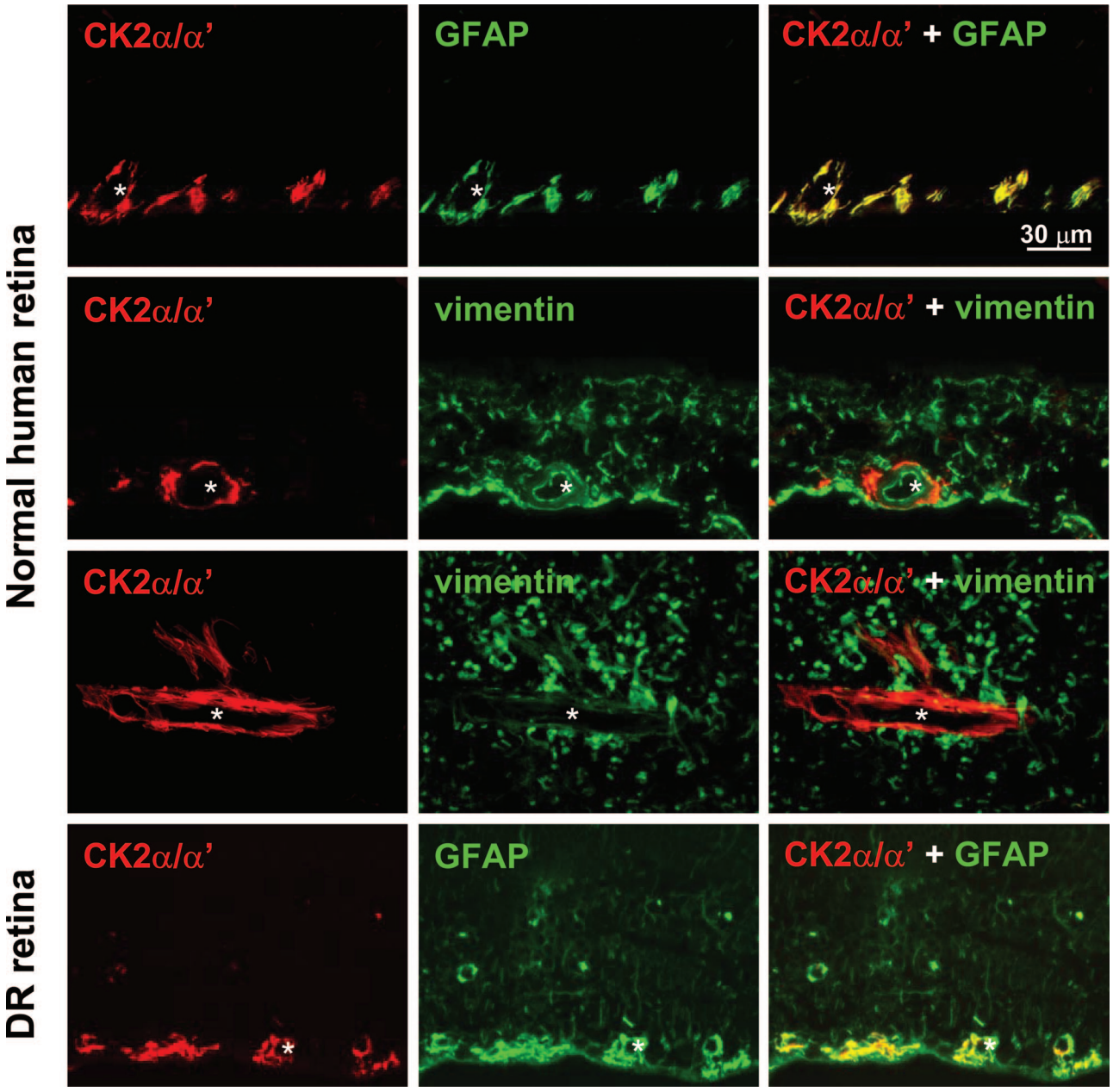

Figure 1. CK2α/α' subunits are predominantly expressed in retinal astrocytes. **Top row:** Retina from a nondiabetic patient; double-immunohistochemical staining. CK2α/α' completely co-distributes in the nerve fiber layer of the inner retina with retinal astrocyte marker, GFAP (**right**, double staining). **Second row:** Retina from a nondiabetic patient. Anti-CK2α/α' mAb 1AD9 labels glial cell projections that closely appose blood vessels. No co-distribution with Müller cell marker, vimentin, is seen with double staining (**right**). **Third row:** Retina from a nondiabetic patient. On oblique section, it is clearly seen that CK2-positive astrocytes wrap around a blood vessel; Müller cell processes positive for vimentin are more distant from the vessel (**right**, double staining). **Bottom row:** Retina from a patient with DR. Müller cell processes marked by vimentin immunoreact with anti-GFAP antibody as well, indicating up-regulation of GFAP in reactive glial cells. However, CK2α/α' does not highlight Müller cells and is revealed only in astrocytes. **Asterisks** mark blood vessels.

anti-CK2 subunit antibodies. Specific bands of 48 kd, 40 kd, and 26 kd were revealed corresponding to α, α', and β subunits, respectively (not shown), indicating significant expression of all three CK2 subunits in the human retina.

In cultured astrocytes from human optic nerve head explants or from human brain (NHA or HAST040), immunostaining for CK2α/α' co-distributed with that of GFAP (Figure 4, A–C; HAST040 cells) suggesting association of CK2 with the cytoskeleton. A substantial fraction of CK2α/α' and GFAP immunoreactivity in cultured astrocytes (Figure 4, A–E) had perinuclear localization similar to that of microtubule-organizing center described earlier for astrocytes.[42] In cultured human microvascular endothelial cells, CK2α/α' immunostaining was more diffusely distributed in the cytoplasm than in cultured astrocytes although it could also be co-distributing with the cytoskeleton (Figure 4F). Semiquantitative Western analyses did not reveal significant differences in the level of CK2α and CK2α' between cultured human astrocytes and endothelial cells when evaluated relative to β-tubulin expression (not shown).

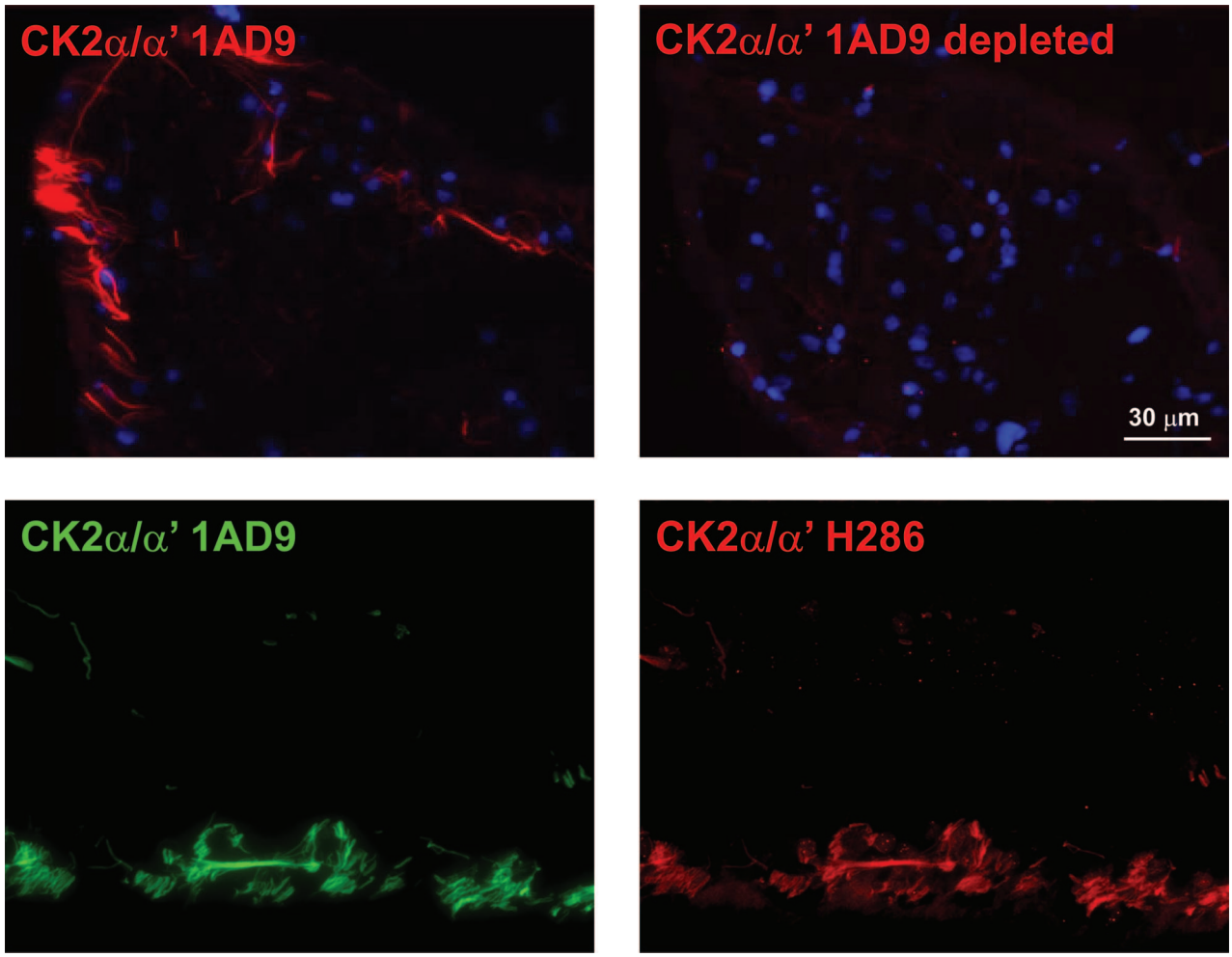

Figure 2. Specificity of immunoreactivity of human retinal astrocytes with mAb 1AD9. **Top row:** A dramatic decrease of astrocyte immunostaining after depletion of anti-CK2α/α' antibody 1AD9 by incubation with a peptide comprising the specific epitope. **Bottom row:** Complete co-distribution of retinal CK2 staining using mAb 1AD9 and a polyclonal antibody H-286 used for rodent studies.

RT-PCR Analysis of CK2 Subunit Expression in Human Retina

By RT-PCR, specific bands corresponding to all three subunits were revealed in retinal tissue (Figure 5A). Because CK2α has different splice variants,[43] their expression was analyzed separately. With primers in exons 1 and 4 (Figure 5A, lane 2) two bands were revealed (minor at 572 bp and major at 455 bp). Cloning and sequencing showed that the 572-bp band contained all exons between 1 and 4 (Figure 5C) corresponding to transcript variant 1 (GenBank accession number NM_177559).[43] The major 455-bp band lacked exon 2 (Figure 5C) corresponding to transcript variant 2 (GenBank accession number NM_001895).[43] Both transcripts give rise to the same size protein because translation starts in exon 3 (Figure 5C). These variants were found in both normal and DR retinas (Figure 5A).

When the number of PCR cycles was increased to 40, a third band at 245 bp was clearly revealed (Figure 5B). By cloning and sequencing, the minor 245-bp band was found to lack exons 2 and 3 (Figure 5C) corresponding to a short transcript variant 3. This variant will yield a smaller protein because the next translation start is in exon 6 (Figure 5C). Variant 3 had not been previously described for CK2α. BLAST search only showed that our sequence (GenBank accession number AY735339) was within an expressed sequence tag (EST; from retinoic acid-treated NT2 human teratocarcinoma; GenBank accession number AU131227). This variant was expressed in both normal and DR retinas (not shown here).

CK2 Expression in Rodent Models of Retinal Neovascularization

In normal mouse retina, CK2α/α' immunoreactivity was also confined to GFAP-positive astrocytes in the nerve fiber layer (Figure 6, top row). Astrocytes of mouse retinas with intraretinal neovascularization showed increased staining for CK2α/α' compared to normoxic control retinas, as well as for GFAP (Figure 6, second row). CK2-positive astrocytes were often seen in close apposition to the new superficial intraretinal vessels next to the inner limiting membrane (Figure 6, third row, arrows). After treatment of mice in the OIR model with emodin, a CK2 inhibitor, intraretinal neovascularization was mark-

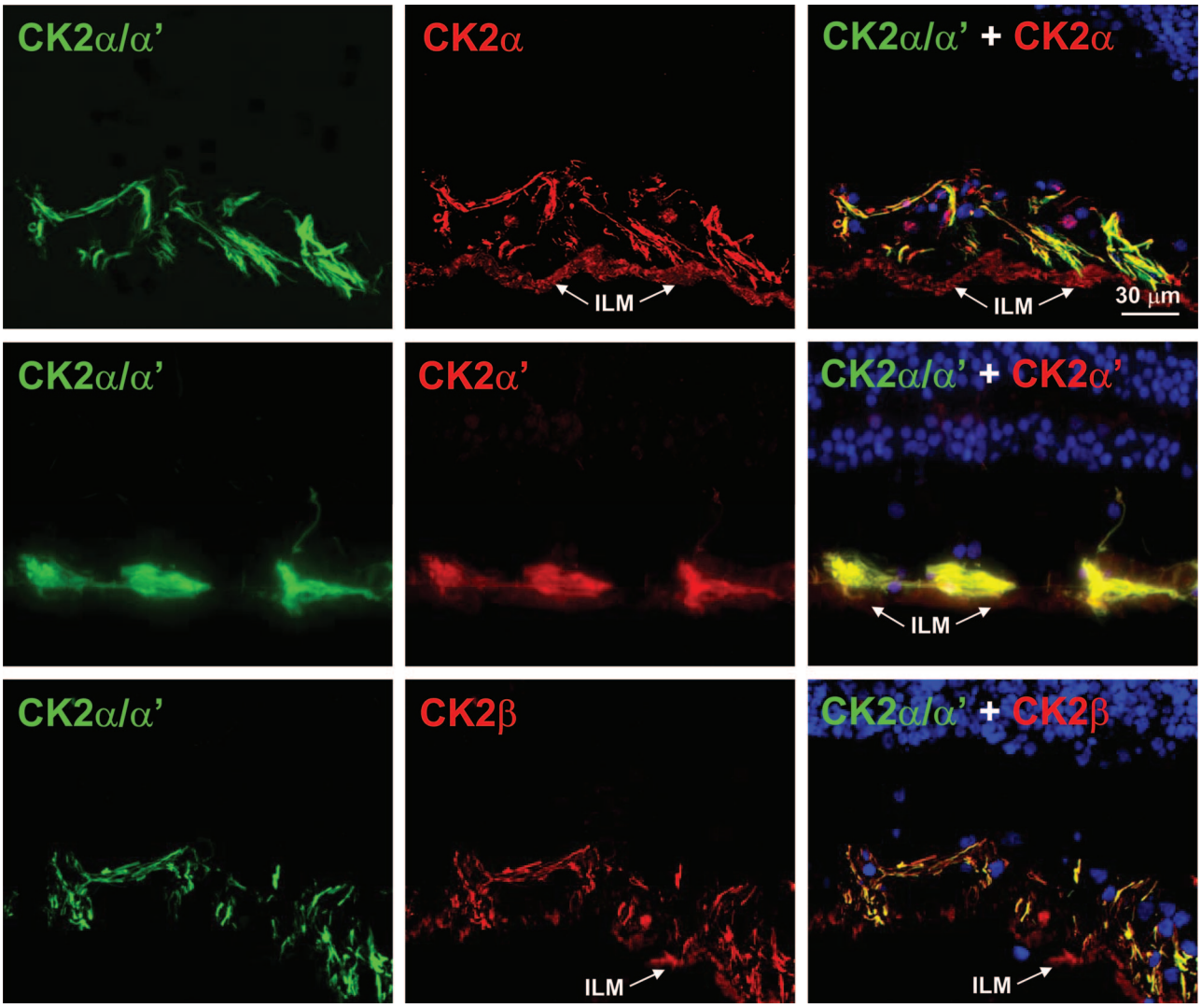

Figure 3. Human retinal astrocytes express α, α', and β subunits of CK2. Only astroglial cells are stained by polyclonal rabbit antibodies to subunit-specific peptides. Each of these antibodies [anti-α (**top row**), anti-α' (**middle row**), and anti-β (**bottom row**)] co-distribute with 1AD9 mAb (CK2α/α') used here as an astrocyte marker (**left**). Some nonspecific background staining by polyclonal antibodies can be seen in the inner limiting membrane (ILM) and occasionally, in the cell nuclei of the inner nuclear layer. Normal human retina is shown. **Right:** Triple label images, DAPI staining shows nuclei.

edly reduced and CK2α/α' staining was similar to normal (Figure 6, bottom row).

In the Müller cells of neovascularized OIR retinas, GFAP immunoreactivity was also detected but CK2 staining was absent (Figure 7, top row). Thus, intraretinal neovascularization in the mouse OIR appears to be associated with an increase of CK2 in astrocytes but not in Müller cells. In accordance with previous data,[37] preretinal vessels contained no glial elements as revealed by lack of staining for CK2, GFAP (Figure 7, bottom row), or vimentin (not shown). This result was obtained in both mouse strains: the less angiogenic C57BL/6J and the more angiogenic 129S3/SvIM. In line with earlier data from a kitten ROP model,[44] preretinal vessels showed positive staining for desmin (Figure 7, bottom right) and α-smooth muscle actin, markers of vascular mural cells. In the rat ROP model, we also observed an increase in CK2 immunoreactivity in areas of intraretinal neovascularization compared to control normoxic retinas (not shown), although not as significant as in the mouse model.

CK2 expression changes during neovascularization development in OIR model were quantified by QPCR and Western analyses of mouse retinas. By QPCR, the levels of CK2α, CK2α', and CK2β mRNAs in day P13 OIR retinas were all 20 to 25% higher than in day P13 normoxic retinas, whereas in day P17 retinas OIR samples showed a similar decrease for all CK2 subunits compared to normoxic controls (Figure 8A).

Western analyses of mouse retinal extracts did not show significant differences in the amount of CK2α between normoxic and oxygen-treated retinas (Figure 8B). At the same time, a significant twofold increase in the amount of GFAP in OIR compared to normoxic mouse retinas was revealed by Western analyses (Figure 8B). This can be explained by up-regulation of GFAP expression not only in astrocytes but also in Müller cells, the latter being one of the main retinal cell types.

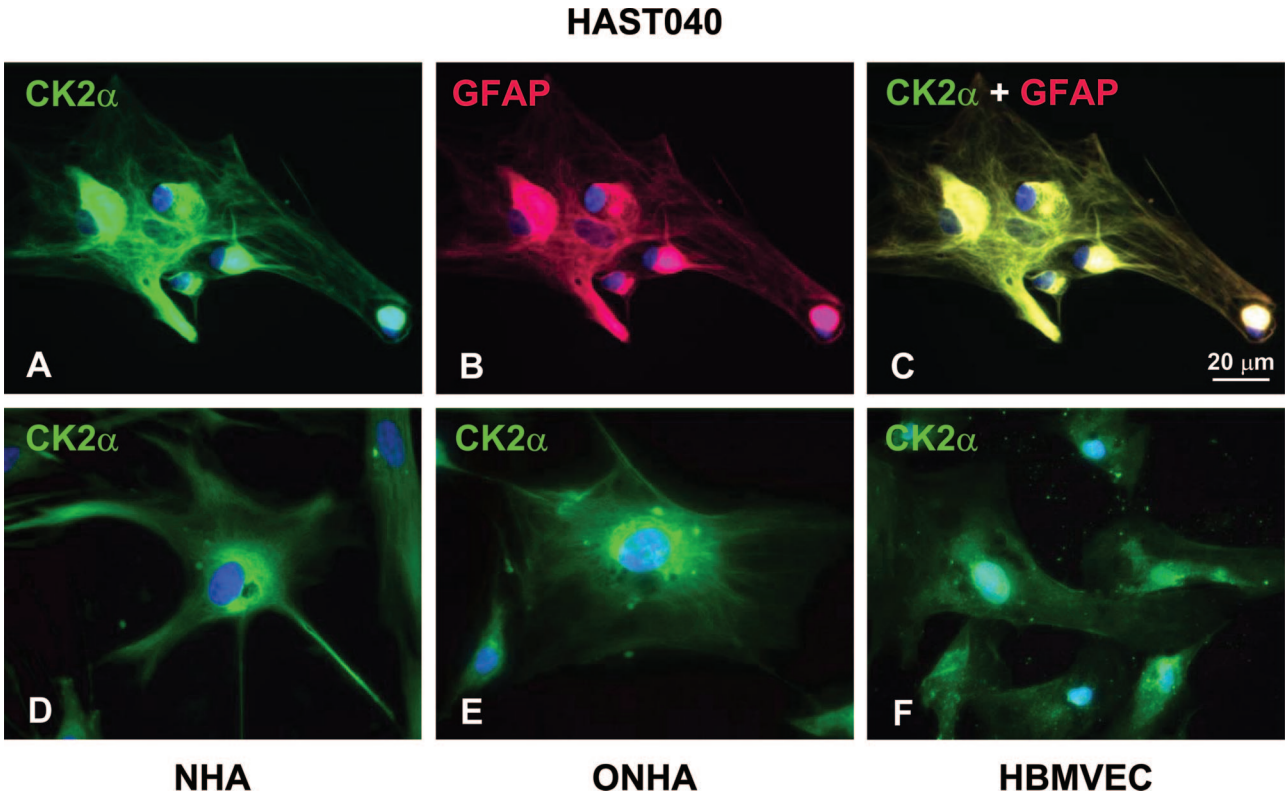

Figure 4. CK2 immunostaining of human astrocyte and endothelial cultures. **A–C:** Embryonic brain astrocytes HAST040. **A:** Perinuclear areas stain strongly for CK2. **B:** Same structures stain for GFAP. **C:** Significant co-distribution of CK2 and GFAP revealed by color overlap (yellow). **D** and **E:** Staining of adult astrocytes from brain (**D**, NHA) and optic nerve head (**E**, ONHA) reveals similar albeit less intense staining for CK2. **F:** Brain microvascular endothelial cells (HBMVECs) display diffuse cytoplasmic staining for CK2. In all plates, nuclei are counterstained with DAPI (blue color).

Combined Treatment of Mouse OIR with CK2 Inhibitors and Somatostatin Analogs

It was of interest to determine whether the effect of CK2 inhibitors would be enhanced if they were combined with other anti-angiogenic drugs with different mechanisms of action. We chose the somatostatin analog octreotide as one such drug. Alone, octreotide was able to reduce preretinal neovascularization in the OIR model by ~67% at 5 mg/kg/day (Figure 9). When just 1 mg/kg/day octreotide was combined with 30 mg/kg/day emodin, the same extent of inhibition was observed as with 5 mg/kg/day octreotide alone (Figure 9). A similar significant increase of inhibition efficiency was obtained when 1 mg/kg/day octreotide was combined with 30 mg/kg/day TBB, the most specific CK2 inhibitor to date,[27] although the effect was slightly less pronounced than with emodin (Figure 9). Therefore, different anti-angiogenic compounds may exert an increased reduction of neovascularization when applied in combination, which may be important for future clinical applications. All treatments mainly reduced preretinal neovascularization.

Discussion

Despite the ubiquitous nature of CK2, no data were available on its occurrence in the eye tissues. Here we report for the first time on the expression of CK2 in human and

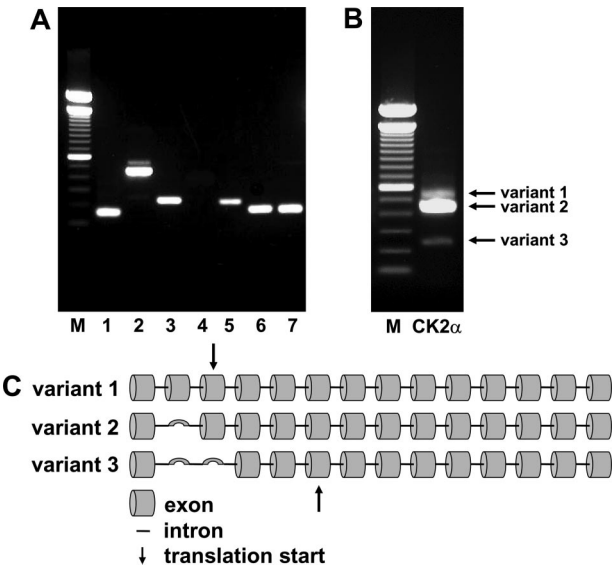

Figure 5. RT-PCR analysis of CK2 subunit expression in normal human retina. **A: Lane 1**, CK2α 3′-end, 151 bp (variants 1, 2, 3); **lane 2**, CKα exons 1 to 4, 562, 446, 245 bp (variants 1, 2, 3, respectively), the 245-bp band (variant 3) is barely visible here; **lane 3**, CKα variant 2, 214 bp (primers in the boundaries of exons 1/3 and 3/4); **lane 4**, CKα variant 3, 191 bp; absent here (primers in the boundaries of exons 1 and 1/4); **lane 5**, CK2α variant 1, 225 bp (primers in exons 2 to 3); **lane 6**, α′ 3′-end, 163 bp; **lane 7**, β 3′-end, 158 bp; M, 100-bp DNA ladder. **B:** A 40-cycle RT-PCR of CK2α with primers in the 3′ end (as in **A**, **lane 1**). Bands corresponding to all three variants (1 at 562 bp, 2 at 446 bp, and 3 at 245 bp) are seen. Variant 2 is the major one in the retina. **C:** Schematic of CK2α splice variants. Variant 3 gives rise to a shorter form because the initial translation start site is spliced out.

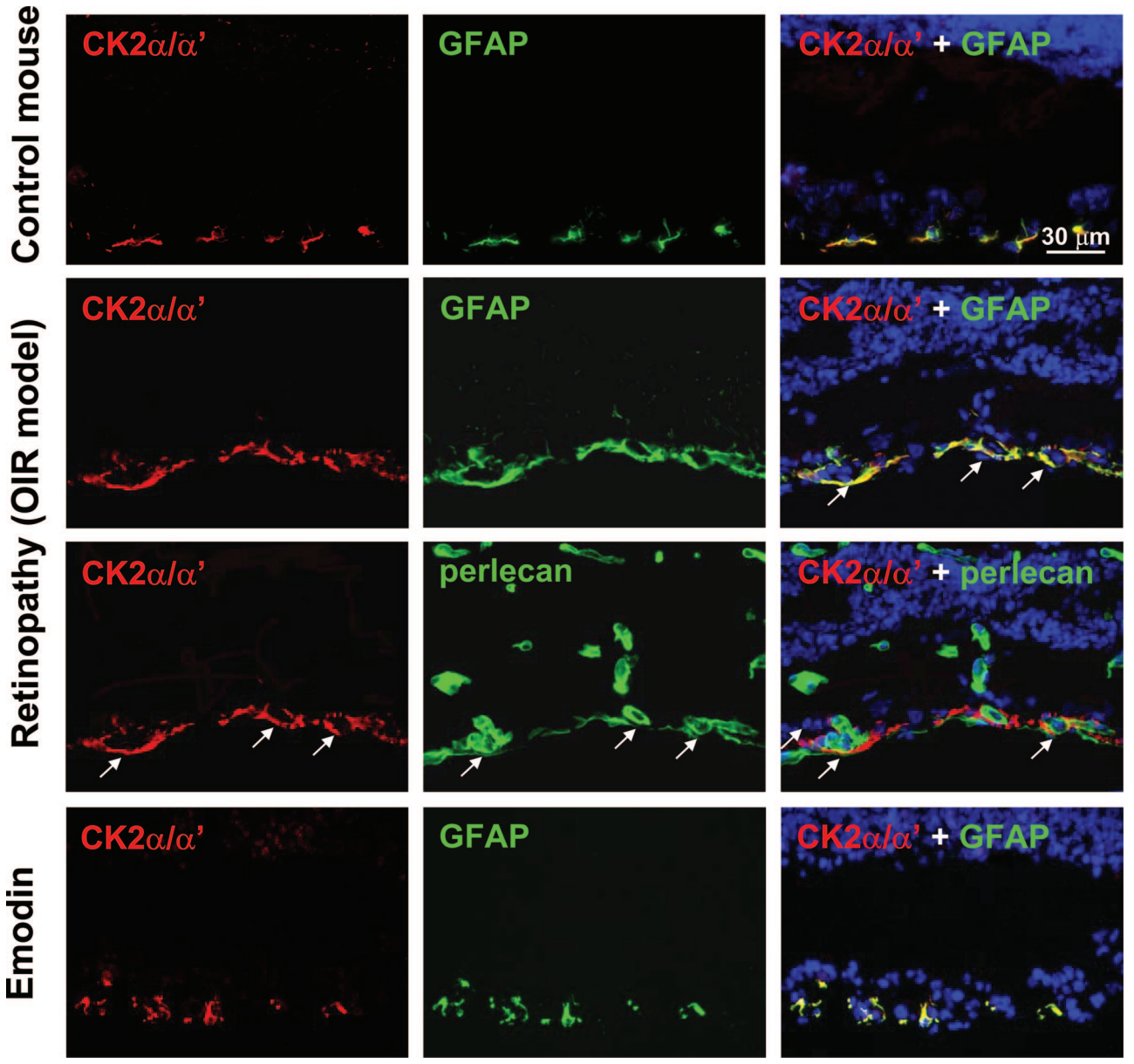

Figure 6. CK2α/α' expression is increased in the mouse OIR model. Control retina (**top row**)**:** Anti-CK2α/α' antibody labels astrocytes as does GFAP. OIR model (**second** and **third rows**; same section): CK2 staining is increased in retinopathy, in areas of neovascularization. CK2 staining primarily co-distributes with GFAP (**second row**, **right**; yellow color). In neovascularized areas, CK2-positive astrocytes ensheathe new blood vessels (**third row**; section was photobleached and then restained for basement membrane protein, perlecan, to highlight viable blood vessels,[39] **arrows**). Emodin-treated retina (**bottom**)**:** after treatment, CK2- and GFAP-staining patterns are similar to normal. DAPI staining shows nuclei. **Right:** Triple label images.

rodent retina. Surprisingly, CK2 can be detected as a protein by immunohistochemistry in only one type of retinal cells, that is, in the astrocytes. Other retinal cells might express CK2 at a significantly lower level, or have the epitopes recognized by the anti-CK2 antibodies masked, and, thus, cannot be detected by standard immunohistochemical method used in our studies. Positive staining of retinal vascular endothelial cells for CK2 α and β after pretreatment with 0.05% sodium dodecyl sulfate (A.A. Kramerov, unpublished) indicates that conformational features may influence CK2 immunoreactivity.

The expression of GFAP is known to be down-regulated in the astrocytes of human DR retinas[42] as well as in animal models of DR.[45,46] In diabetic rats, a decrease in astrocytic GFAP immunoreactivity was accompanied by an up-regulation of GFAP in Müller cells,[45] which is considered one of the main features of reactive gliosis.[46] GFAP up-regulation in Müller cells was also documented in human retinas from diabetic and DR patients.[40,41]

We also observed significant GFAP immunoreactivity in human Müller glia of diabetic retinas. However, CK2 immunoreactivity was not detected in Müller cells of either normal or diabetic retinas. These data suggest that up-regulation of CK2 is not part of reactive gliosis, contrary to GFAP, and that CK2 can only be detected in astrocytes. CK2 may thus be considered as one of the most reliable immunohistochemical markers to date for retinal astrocytes.

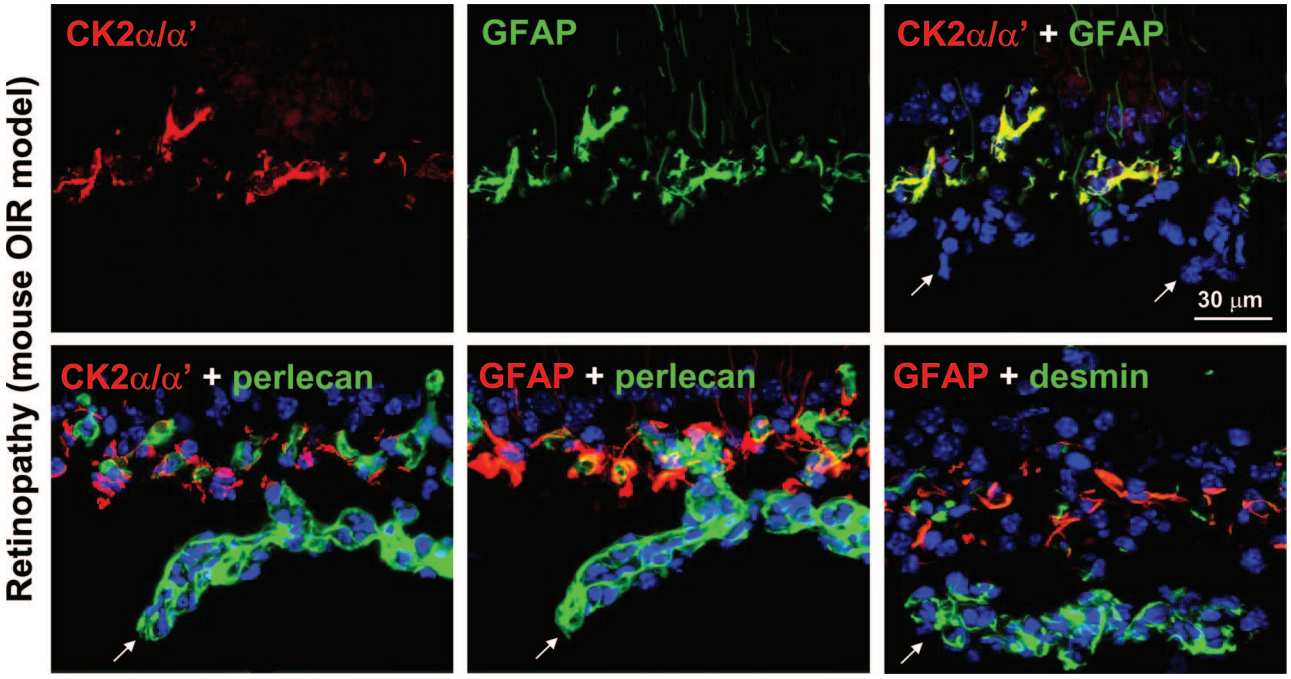

Figure 7. CK2α/α' is not expressed around preretinal neovessels in the mouse OIR model. **Top row:** Strong staining of astrocytes for CK2α/α' and GFAP. Both proteins co-distribute in astrocytes (**right**, yellow color) but GFAP is also seen in Müller cell transverse projections (**right**, green color). Nuclei of glial marker-negative preretinal vessels stained with DAPI are marked with **arrows**. **Bottom row:** Astrocytes positive for CK2 and GFAP (**left** and **middle**) only surround intraretinal but not preretinal (**arrows**) vessels. Preretinal vessels are positive for mural cell marker, desmin (**right**). Triple label immunohistochemistry.

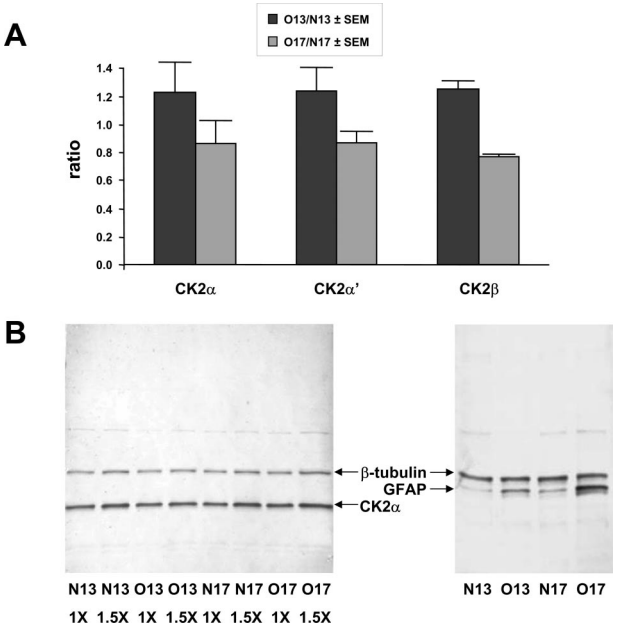

Figure 8. Quantitative analysis of CK2 expression in the OIR model. **A:** QPCR reveals ~20% increase of message levels of all three CK2 subunits in the OIR group (O) compared to normoxic controls (N) at day P13. At day P17, CK2 levels in OIR group dropped to ~80% of normoxic controls group. Bars, mean ± SD (three experiments). **B:** Western blot analysis of retinal extracts for CK2α from the same samples as in **A**. **Left:** Lack of change in CK2α levels in OIR (O) versus normoxic (N) retinas compared to β-tubulin at days P13 and P17. 1× and 1.5× loading amounts for each sample are presented to show the reproducibility and sensitivity. **Right:** GFAP amount is increased approximately twofold in the OIR (O) versus normoxic (N) retinas compared to β-tubulin at days P13 and P17.

Our data on cultured human astrocytes further suggest that CK2 may be closely associated with the cytoskeleton including GFAP-containing intermediate filaments. Interestingly, tubulin, vimentin, and microtubule-associated protein 1B (MAP 1B) are known substrates for CK2,[47,48] but so far there are no data on phosphorylation of GFAP by CK2. Possible CK2-mediated phosphorylation of cytoskeletal proteins in retinal astrocytes and/or endothelial

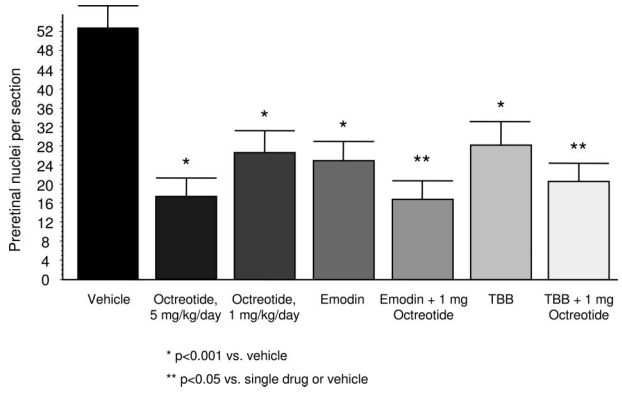

Figure 9. Combination of emodin or TBB with octreotide more efficiently reduces mouse retinal neovascularization than any single drug alone. Counts of preretinal nuclei as a measure of neovascularization in various groups of mice are shown. Intraperitoneal treatment with 30 mg/kg/day of emodin reduced retinal neovascularization by ~57%, and with TBB, by 46%. Treatment with 5 mg/kg/day of octreotide yielded ~67% reduction, and with 1 mg/kg/day of octreotide, ~50% reduction. Emodin combined with 1 mg/kg/day octreotide reduced neovascularization by 69%, and TBB combined with 1 mg/kg/day octreotide, by 61%. Ten sections per eye from each mouse were counted. Five mice were used per each group in three independent experiments. Vehicle represents emodin solvent because octreotide solvent was just PBS. Bars, mean ± SD. $^{*}P < 0.001$ versus vehicle, $^{**}P < 0.05$ versus single drug or vehicle.

cells that may cause changes in cell shape, motility, and migration is an interesting issue for future studies.

We further characterized CK2 mRNA pattern in retina by RT-PCR. CK2 is represented in the human genome by four genes coding for three individual subunits, with the fourth sequence being an intronless CK2α pseudogene.[49–52] A recently identified CK2α'' subunit is a larger variant of α that has a translated Alu sequence at the C-terminus.[53] CK2α has several splice variants.[43] The two larger ones (variants 1 and 2) give rise to the same full-length protein. Our RT-PCR analysis has also revealed a third transcript (variant 3, GenBank accession number AY735339) that is shorter than the other two. The same sequence has been previously deposited to GenBank as an EST (GenBank accession number AU131227). Sequencing revealed that it is missing exons 2 and 3. Because exon 3 has the translation start site, variant 3 would thus code for a smaller protein due to translation starting in exon 6. Variant 3 was expressed at very low levels in human retina. Possibly, it has low levels in other tissues as well because a shorter α subunit has not been detected previously by Western blot.

It was not obvious whether the human diabetic retinas that we analyzed had active neovascularization because of the anti-diabetic treatment, including photocoagulation, and incomplete data in some cases. To identify possible changes in CK2 expression patterns associated with neovascularization, we turned to mouse OIR and rat ROP models of proliferative retinopathy. In rodent models, we found gliosis in areas of intraretinal neovascularization in the vicinity of inner limiting membrane, which appeared to have two components, astrogliosis and Müller cell gliosis, in accordance with previous data.[54] In astrogliosis, increased GFAP staining of astrocytes is also accompanied by brighter CK2 staining. In contrast, Müller cell gliosis, characterized by both noticeable expression of GFAP and significant increase of vimentin staining of Müller cell processes close to the intraretinal vessels, did not include any detectable expression of CK2. Thus, CK2 expression detected by immunohistochemistry appears to be a specific feature of astrocytes in normal and diabetic retinas, as well as in hypoxia-induced neovascularization.

To quantify changes in CK2 expression in mouse OIR model, both QPCR and Western analyses were used. When normoxic and OIR mouse retinas were compared, a modest increase of CK2 subunit expression was found by QPCR at day P13 when VEGF peaks in the retinas of animals subjected to OIR protocol.[55] However, levels of all CK2 subunits were slightly down-regulated in the OIR group at day P17 that corresponds to maximum neovascularization before the beginning of new vessel regression by apoptosis. A transient increase in expression with similar time course was previously documented in this model for $VEGF_{120}$ and its receptor Flk-1/VEGFR2.[56,57]

Western analyses did not show substantial changes in the amount of CK2α in OIR versus normoxic retinas (Figure 8). Presumably, quantifying CK2, an ubiquitous protein kinase, in a pooled sample with contributions from all of the retinal cells makes it very difficult to discover its increased amount resulting only from its up-regulation in astrocytes, a minor fraction of retinal cells. Another possibility may be a lower turnover rate of CK2α subunit compared to its mRNA that makes it more difficult to detect changes in the net retinal amount of CK2α at the protein level. Conversely, GFAP expression is normally restricted to astrocytes but is up-regulated in OIR in abundant Müller glial cells,[58] which, in accordance with the above reasoning, allows one to quantify changes in GFAP levels. Indeed, Western analyses revealed a significant increase in GFAP expression in OIR compared to normoxic mouse retinas (Figure 8).

Specific inhibition of CK2 leads to a significant decrease of neovascularization in mouse OIR[27] and to an apparent suppression of astrogliosis resulting in normal levels of GFAP and CK2 expression, and, surprisingly, to a decreased GFAP immunoreactivity in Müller cells. One can assume that hypoxia causes up-regulation of CK2 in astrocytes that promotes neovascularization accompanied by increased GFAP expression both in astrocytes and Müller cells, and this sequence of events is blocked by CK2 inhibition.

The data suggest that there are two types of retinal neovascularization. The first one is intraretinal neovascularization, which is similar to retinal angiogenesis during development. It involves astrogliosis[54,59] and sprouting of superficial retinal vessels guided by astrocytes that migrate ahead of the growing vessels and invest them.[3] The second type of neovascularization is vitreal, or preretinal, neovascularization. It may develop by a different mechanism involving ischemia-driven local depletion of astrocytes in the vicinity of inner limiting membrane by apoptosis and a relief of endothelial cells from astrocytic constraint to the retina.[60] It may be suggested that when insufficient astrocytes can no longer constrain endothelial cells, neovessels start forming as buds, or microaneurysms, and preretinal vessels may grow through the breaches of glia limitans and inner limiting membrane into the vitreous.

Our data on mouse OIR suggest that CK2 might play an important role in both types of retinal neovascularization. Here we report that in OIR, CK2 immunostaining is up-regulated in astrocytes near superficial retinal blood vessels during intraretinal neovascularization. CK2 inhibitors blocked ischemia-induced formation of new superficial intraretinal vessels and decreased CK2 immunostaining of astrocytes associated with new retinal vessels. One can hypothesize that emodin and TBB block CK2 activity primarily in astrocytes and thus may inhibit intraretinal neovascularization.

At the same time, emodin and TBB also significantly reduce intravitreal neovascularization as we have reported earlier.[27] However, CK2 or GFAP expression was not observed in preretinal vessels in the OIR retinas, in accordance with previous studies that reported lack of glial cells in preretinal neovascular tufts.[37,59] Interestingly, glial elements were also absent in neovascularized sea fans[61] in human ischemia-driven sickle cell retinopathy (A.A. Kramerov, A.V. Ljubimov, and G.A. Lutty, unpublished). One can propose that it is inhibition of CK2 in endothelial cells that causes a decrease of their proliferation and migration thus blocking vitreal neovasculariza-

tion. Alternatively, in OIR, expansion of astrocytes expressing CK2 in the inner retina may promote extensive proliferation of endothelial cells, which then breach through inner limiting membrane causing vitreal neovascularization. In this case, CK2 inhibitor action on both proliferating astrocytes and endothelial cells will again result in preventing vitreal neovascularization. Considering these possibilities one may suggest that CK2 inhibitors could affect CK2 activity both in endothelial cells and in astrocytes leading to blocking intravitreal, as well as intraretinal neovascularization.

After octreotide treatment, retinal CK2 patterns were similar to those after emodin treatment. Octreotide can block proliferation of various cell types including endothelial cells and astrocytes.[62,63] Therefore, somatostatin analogs may inhibit neovascularization by affecting both astrocytes and endothelial cells, similar to CK2 inhibitors.

CK2 may be involved in retinal angiogenesis by mediating cell survival in hypoxic conditions. Hypoxia may cause regional degeneration of retinal astrocytes as revealed by down-regulation of GFAP expression in animal ROP[64] and streptozotocin-induced diabetes[54] models, but after hypoxic damage, astrocytes recolonize the retina to restore blood-retina barrier and take part in vasoproliferation.[64] Astrocytes produce VEGF and fibroblast growth factor-2 that are survival factors for retinal endothelial cells and could rescue them from hypoxia-induced apoptosis.[16,22] CK2 is an anti-apoptotic agent[25,65,66] that may allow survival of retinal astrocytes in ischemia, which would promote retinal revascularization through astrocytic VEGF expression, as was shown in the mouse OIR.[58]

CK2 could also control retinal neovascularization via anti-angiogenic PEDF.[67] PEDF from plasma could be phosphorylated by secreted CK2 *in vivo* and CK2 phosphorylation site mutant of PEDF showed enhanced anti-angiogenic activity.[68] Up-regulation of CK2 expressed and possibly secreted by astrocytes may thus lead to increased phosphorylation of PEDF released by retinal pigment epithelium and Müller cells. This would cause a decrease in anti-angiogenic activity of PEDF and promote neovascularization. Conversely, CK2 inhibition will result in under-phosphorylated PEDF, thus enhancing its anti-angiogenic activity and blocking neovascularization.

Combination therapy is a mainstream approach for treatment of cancer, AIDS, and other systemic diseases.[69,70] Currently, many anti-angiogenic compounds are being tested in animal models of retinal neovascularization and in patients in an attempt to prevent DR progression, most often, one at a time,[71–74] but so far have demonstrated only limited efficacy. This incomplete inhibition may be due in part to the multifactorial nature of DR, making targeting a single cellular mechanism inadequate. Therefore, we started examining combination therapy approach for inhibiting retinal neovascularization. In accordance with previous data, each of the two drugs, somatostatin analog, octreotide,[75] and CK2 inhibitors, emodin and TBB,[27] inhibited retinopathy in the mouse OIR model. Moreover, we found for the first time that the effect of the drug combination was significantly stronger than of either single drug. The use of emodin allowed us to achieve the same inhibition with 1 mg/kg/day octreotide as was achieved with 5 mg/kg/day octreotide alone, with TBB being somewhat less effective. This additive effect may be very important in the clinical setting, because only maximally tolerated doses of octreotide could significantly retard the development of PDR.[63,76]

What could be the mechanism of enhanced combined effect of octreotide and emodin or TBB in inhibiting OIR? Such additive result may be due to supposedly nonoverlapping networks of signaling pathways targeted by these two types of inhibitors. CK2 inhibition may negatively impact angiogenic pathways involving Ras/Raf/MEK kinases, Akt/protein kinase-B, and protein kinase-C.[27] However, CK2 was not reported to interact with the JAK/STAT signaling pathway[77–79] or $p27^{kip1}$, cell growth inhibitor,[80] that are major mediators of anti-angiogenic effects of somatostatin analogs. At the same time, CK2 inhibitors and somatostatin analogs would block some common pathways, eg, p53 and Ras/Raf/MEK kinases, which may explain their moderate additive effect. Overall, combination therapy for pathological angiogenesis involving agents with different mechanisms of action may soon become a promising treatment approach in cancer, DR, and macular degeneration.

While this article was in review, new data were published showing a fivefold stimulation of CK2 activity by hypoxia. Moreover, inhibition of CK2 by TBB in cultured hepatoma cells resulted in suppression of hypoxia-inducible factor-1 activity and VEGF production.[81] These data, together with our observations, allow us to hypothesize about the role of CK2 as a regulator of hypoxia-inducible factor-1-mediated hypoxia-driven angiogenesis.

Acknowledgments

We thank A. Aoki for excellent technical help; Sergio Caballero, Dr. Lynn C. Shaw, and Dr. Aqeela Afzal (Department of Pharmacology, University of Florida, Gainesville, FL) for performing some animal experiments and the gift of cultured cells; Dr. Eva Engvall (The Burnham Institute, La Jolla, CA) for anti-laminin antibodies; Dr. Gerard A. Lutty (Wilmer Ophthalmological Institute, Johns Hopkins University, Baltimore, MD) for kindly providing sections of retinas from sickle cell retinopathy patients; Drs. M. Rosario Hernandez and Olga Agapova (Department of Ophthalmology and Visual Sciences, Washington University, St. Louis, MO) for cultures of human ONH astrocytes used in some experiments; and Prof. Lorenzo A. Pinna (Dipartimento di Chimica Biologica, Universita di Padova, Padova, Italy) for helpful discussions and suggestions.

References

1. Fruttiger M: Development of the mouse retinal vasculature: angiogenesis versus vasculogenesis. Invest Ophthalmol Vis Sci 2002, 43:522–527
2. McLeod DS, Crone SN, Lutty GA: Vasoproliferation in the neonatal

dog model of oxygen-induced retinopathy. Invest Ophthalmol Vis Sci 1996, 37:1322–1333
3. Gariano RF: Cellular mechanisms in retinal vascular development. Prog Retin Eye Res 2003, 22:295–306
4. Grant MB, May WS, Caballero S, Brown GA, Guthrie SM, Mames RN, Byrne BJ, Vaught T, Spoerri PE, Peck AB, Scott EW: Adult hematopoietic stem cells provide functional hemangioblast activity during retinal neovascularization. Nat Med 2002, 8:607–612
5. Sengupta N, Caballero S, Mames RN, Timmers AM, Saban D, Grant MB: Preventing stem cell incorporation into choroidal neovascularization by targeting homing and attachment factors. Invest Ophthalmol Vis Sci 2005, 46:343–348
6. Otani A, Kinder K, Ewalt K, Otero FJ, Schimmel P, Friedlander M: Bone marrow-derived stem cells target retinal astrocytes and can promote or inhibit retinal angiogenesis. Nat Med 2002, 8:1004–1010
7. Grant MB, Afzal A, Spoerri P, Pan H, Shaw LC, Mames RN: The role of growth factors in the pathogenesis of diabetic retinopathy. Expert Opin Investig Drugs 2004, 13:1275–1293
8. Saint-Geniez M, D'Amore PA: Development and pathology of the hyaloid, choroidal and retinal vasculature. Int J Dev Biol 2004, 48:1045–1058
9. Thurston G, Gale NW: Vascular endothelial growth factor and other signaling pathways in developmental and pathologic angiogenesis. Int J Hematol 2004, 80:7–20
10. Bikfalvi A: Platelet factor 4: an inhibitor of angiogenesis. Semin Thromb Hemost 2004, 30:379–385
11. Eichler W, Yafai Y, Keller T, Wiedemann P, Reichenbach A: PEDF derived from glial Müller cells: a possible regulator of retinal angiogenesis. Exp Cell Res 2004, 299:68–78
12. Frank RN: Diabetic retinopathy. N Engl J Med 2004, 350:48–58
13. Fong DS, Aiello LP, Ferris III FL, Klein R: Diabetic retinopathy. Diabetes Care 2004, 27:2540–2553
14. Cai J, Boulton M: The pathogenesis of diabetic retinopathy: old concepts and new questions. Eye 2002, 16:242–260
15. Caldwell RB, Bartoli M, Behzadian MA, El-Remessy AE, Al-Shabrawey M, Platt DH, Caldwell RW: Vascular endothelial growth factor and diabetic retinopathy: pathophysiological mechanisms and treatment perspectives. Diabetes Metab Res Rev 2003, 19:442–455
16. Alon T, Hemo I, Itin A, Pe'er J, Stone J, Keshet E: Vascular endothelial growth factor acts as a survival factor for newly formed retinal vessels and has implications for retinopathy of prematurity. Nat Med 1995, 1:1024–1028
17. Leske DA, Wu J, Fautsch MP, Karger RA, Berdahl JP, Lanier WL, Holmes JM: The role of VEGF and IGF-1 in a hypercarbic oxygen-induced retinopathy rat model of ROP. Mol Vis 2004, 10:43–50
18. Pierce EA, Avery RL, Foley ED, Aiello LP, Smith LE: Vascular endothelial growth factor/vascular permeability factor expression in a mouse model of retinal neovascularization. Proc Natl Acad Sci USA 1995, 92:905–909
19. Gerhardt H, Golding M, Fruttiger M, Ruhrberg C, Lundkvist A, Abramsson A, Jeltsch M, Mitchell C, Alitalo K, Shima D, Betsholtz C: VEGF guides angiogenic sprouting utilizing endothelial tip cell filopodia. J Cell Biol 2003, 161:1163–1177
20. Campochiaro PA: Retinal and choroidal neovascularization. J Cell Physiol 2000, 184:301–310
21. Mi H, Haeberle H, Barres BA: Induction of astrocyte differentiation by endothelial cells. J Neurosc 2001, 21:1538–1547
22. Yamada H, Yamada E, Ando A, Seo MS, Esumi N, Okamoto N, Vinores M, LaRochelle W, Zack DJ, Campochiaro PA: Platelet-derived growth factor-A-induced retinal gliosis protects against ischemic retinopathy. Am J Pathol 2000, 156:477–487
23. Litchfield DW: Protein kinase CK2: structure, regulation and role in cellular decisions of life and death. Biochem J 2003, 369:1–15
24. Pinna LA: The raison d'être of constitutively active protein kinases: the lesson of CK2. Acc Chem Res 2003, 36:378–384
25. Unger GM, Davis AT, Slaton JW, Ahmed K: Protein kinase CK2 as regulator of cell survival: implications for cancer therapy. Curr Cancer Drug Targets 2004, 4:77–84
26. Olsten ME, Litchfield DW: Order or chaos? An evaluation of the regulation of protein kinase CK2. Biochem Cell Biol 2004, 82:681–693
27. Ljubimov AV, Caballero S, Aoki A, Grant MB, Castellon R: Involvement of protein kinase CK2 in angiogenesis and retinal neovascularization. Invest Ophthalmol Vis Sci 2004, 45:4583–4591
28. Goueli SA, Davis AT, Arfman E, Vessella R, Ahmed K: Monoclonal antibodies against nuclear casein kinase NII (PK-N2). Hybridoma 1990, 9:609–618
29. Faust M, Jung M, Gunther J, Zimmermann R, Montenarh M: Localization of individual subunits of protein kinase CK2 to the endoplasmic reticulum and to the Golgi apparatus. Mol Cell Biochem 2001, 227:73–80
30. Engvall E, Davis GE, Dickerson K, Ruoslahti E, Varon S, Manthorpe M: Mapping of domains in human laminin using monoclonal antibodies: localization of the neurite-promoting site. J Cell Biol 1986, 103:2457–2465
31. Couchman JR, Ljubimov AV: Mammalian tissue distribution of a large heparan sulfate proteoglycan detected by monoclonal antibodies. Matrix 1989, 9:311–321
32. Nastainczyk W, Issinger OG, Guerra B: Epitope analysis of the MAb 1AD9 antibody detection site in human protein kinase CK2α-subunit. Hybrid Hybridomics 2003, 22:87–90
33. Kobayashi S, Vidal I, Pena JD, Hernandez MR: Expression of neural cell adhesion molecule (NCAM) characterizes a subpopulation of type 1 astrocytes in human optic nerve head. Glia 1997, 20:262–273
34. Saghizadeh M, Kramerov AA, Tajbakhsh J, Aoki AM, Wang C, Chai NN, Ljubimova JY, Sasaki T, Sosne G, Carlson MR, Nelson SF, Ljubimov AV: Proteinase and growth factor alterations revealed by gene microarray analysis of human diabetic corneas. Invest Ophthalmol Vis Sci 2005, 46:3604–3615
35. Penn JS, Henry MM, Tolman BL: Exposure to alternating hypoxia and hyperoxia causes severe proliferative retinopathy in the newborn rat. Pediatr Res 1994, 36:724–731
36. Penn JS, Henry MM, Tolman BL, Wall PT: The range of PaO_2 variation determines the severity of oxygen-induced retinopathy in newborn rats. Invest Ophthalmol Vis Sci 1995, 36:2063–2070
37. Smith LE, Wesolowski E, McLellan A, Kostyk SK, D'Amato R, Sullivan R, D'Amore PA: Oxygen-induced retinopathy in the mouse. Invest Ophthalmol Vis Sci 1994, 35:101–111
38. Grant MB, Caballero S, Mames RN, Shapiro G: Designer drugs: peptidomimetics of somatostatin specifically target ocular neovascularization. Annual Meeting Abstract and Program Planner. Assoc Res Vis Ophthalmol 2005, Abstract 4171
39. Ghosh F, Gjorloff K: Protein kinase C expression in the rabbit retina after laser photocoagulation. Graefes Arch Clin Exp Ophthalmol 2005, 243:803–810
40. Abu-El-Asrar AM, Dralands L, Missotten L, Al-Jadaan IA, Geboes K: Expression of apoptosis markers in the retinas of human subjects with diabetes. Invest Ophthalmol Vis Sci 2004, 45:2760–2766
41. Mizutani M, Gerhardinger C, Lorenzi M: Muller cell changes in human diabetic retinopathy. Diabetes 1998, 47:445–449
42. Salvador-Silva M, Aoi S, Parker A, Yang P, Pecen P, Hernandez MR: Responses and signaling pathways in human optic nerve head astrocytes exposed to hydrostatic pressure in vitro. Glia 2004, 45:364–377
43. Mammalian Gene Collection Program Team: Generation and initial analysis of more than 15,000 full-length human and mouse cDNA sequences. Proc Natl Acad Sci USA 2002, 99:16899–16903
44. Chan-Ling T, Page MP, Gardiner T, Baxter L, Rosinova E, Hughes S: Desmin ensheathment ratio as an indicator of vessel stability: evidence in normal development and in retinopathy of prematurity. Am J Pathol 2004, 165:1301–1313
45. Lieth E, Barber AJ, Xu B, Dice C, Ratz MJ, Tanase D, Strother JM: Glial reactivity and impaired glutamate metabolism in short-term experimental diabetic retinopathy. Penn State Retina Research Group. Diabetes 1998, 47:815–820
46. Rungger-Brandle E, Dosso AA, Leuenberger PM: Glial reactivity, an early feature of diabetic retinopathy. Invest Ophthalmol Vis Sci 2000, 41:1971–1980
47. Janosch P, Kieser A, Eulitz M, Lovric J, Sauer G, Reichert M, Gounari F, Buscher D, Baccarini M, Mischak H, Kolch W: The Raf-1 kinase associates with vimentin kinases and regulates the structure of vimentin filaments. FASEB J 2000, 14:2008–2021
48. Ulloa L, Ibarrola N, Avila J, Diez-Guerra FJ: Microtubule-associated protein 1B (MAP1B) is present in glial cells phosphorylated different than in neurones. Glia 1994, 10:266–275
49. Wirkner U, Voss H, Ansorge W, Pyerin W: Genomic organization and promoter identification of the human protein kinase CK2 catalytic subunit α (CSNK2A1). Genomics 1998, 48:71–78
50. Lozeman FJ, Litchfield DW, Piening C, Takio K, Walsh KA, Krebs EG:

Isolation and characterization of human cDNA clones encoding the α and the α' subunits of casein kinase II. Biochemistry 1990, 29:8436–8447
51. Pyerin W, Ackermann K: Transcriptional coordination of the genes encoding catalytic (CK2α) and regulatory (CK2β) subunits of human protein kinase CK2. Mol Cell Biochem 2001, 227:45–57
52. Pyerin W, Ackermann K: The genes encoding human protein kinase CK2 and their functional links. Prog Nucl Acid Res Mol Biol 2003, 74:239–273
53. Hilgard P, Huang T, Wolkoff AW, Stockert RJ: Translated Alu sequence determines nuclear localization of a novel catalytic subunit of casein kinase 2. Am J Physiol 2002, 283:C472–C483
54. Barber AJ, Antonetti DA, Gardner TW: Altered expression of retinal occludin and glial fibrillary acidic protein in experimental diabetes. The Penn State Retina Research Group. Invest Ophthalmol Vis Sci 2000, 41:3561–3568
55. Simpson DA, Feeney S, Boyle C, Stitt AW: Retinal VEGF mRNA measured by SYBR green I fluorescence: a versatile approach to quantitative PCR. Mol Vis 2000, 6:178–183
56. Smith LE, Kopchick JJ, Chen W, Knapp J, Kinose F, Daley D, Foley E, Smith RG, Schaeffer JM: Essential role of growth hormone in ischemia-induced retinal neovascularization. Science 1997, 276: 1706–1709
57. McColm JR, Geisen P, Hartnett ME: VEGF isoforms and their expression after a single episode of hypoxia or repeated fluctuations between hyperoxia and hypoxia: relevance to clinical ROP. Mol Vis 2004, 10:512–520
58. Gu X, Samuel S, El-Shabrawey M, Caldwell RB, Bartoli M, Marcus DM, Brooks SE: Effects of sustained hyperoxia on revascularization in experimental retinopathy of prematurity. Invest Ophthalmol Vis Sci 2002, 43:496–502
59. McLeod DS, D'Anna SA, Lutty GA: Clinical and histopathologic features of canine oxygen-induced proliferative retinopathy. Invest Ophthalmol Vis Sci 1998, 39:1918–1932
60. Zhang Y, Stone J: Role of astrocytes in the control of developing retinal vessels. Invest Ophthalmol Vis Sci 1997, 38:1653–1666
61. McLeod DS, Merges C, Fukushima A, Goldberg MF, Lutty GA: Histopathologic features of neovascularization in sickle cell retinopathy. Am J Ophthalmol 1997, 124:455–472
62. Feindt J, Mentlein R, Krisch B: Time-dependent influence of the somatostatin analogue octreotide on the proliferation of rat astrocytes and glioma cells. Brain Res 1997, 746:309–313
63. Grant MB, Mames RN, Fitzgerald C, Hazariwala KM, Cooper-DeHoff R, Caballero S, Estes KS: The efficacy of octreotide in the therapy of severe nonproliferative and early proliferative diabetic retinopathy: a randomized controlled study. Diabetes Care 2000, 23:504–509
64. Chan-Ling T, Stone J: Degeneration of astrocytes in feline retinopathy of prematurity causes failure of the blood-retinal barrier. Invest Ophthalmol Vis Sci 1992, 33:2148–2159
65. Ahmad KA, Wang G, Slaton J, Unger G, Ahmed K: Targeting CK2 for cancer therapy. Anticancer Drugs 2005, 16:1037–1043
66. Pinna LA: Protein kinase CK2: a challenge to canons. J Cell Sci 2002, 115:3873–3878
67. Barnstable CJ, Tombran-Tink J: Neuroprotective and antiangiogenic actions of PEDF in the eye: molecular targets and therapeutic potential. Prog Retin Eye Res 2004, 23:561–577
68. Maik-Rachline G, Shaltiel S, Seger R: Extracellular phosphorylation converts pigment epithelium-derived factor from a neurotrophic to an antiangiogenic factor. Blood 2005, 105:670–678
69. Haskell CM (Ed): Cancer Treatment, ed 5. W.B. Saunders Company, Philadelphia, 2001, pp 62–86
70. Habtemariam T, Yu P, Oryang D, Nganwa D, Ayanwale O, Tameru B, Abdelrahman H, Ahmad A, Robnett V: Modelling viral and CD4 cellular population dynamics in HIV: approaches to evaluate intervention strategies. Cell Mol Biol 2001, 47:1201–1208
71. Folkman J: Endogenous angiogenesis inhibitors. APMIS 2004, 112:496–507
72. van Wijngaarden P, Coster DJ, Williams KA: Inhibitors of ocular neovascularization: promises and potential problems. JAMA 2005, 293:1509–1513
73. Speicher MA, Danis RP, Criswell M, Pratt L: Pharmacologic therapy for diabetic retinopathy. Expert Opin Emerg Drugs 2003, 8:239–250
74. Ziche M, Donnini S, Morbidelli L: Development of new drugs in angiogenesis. Curr Drug Targets 2004, 5:485–493
75. Higgins RD, Yan Y, Schrier BK: Somatostatin analogs inhibit neonatal retinal neovascularization. Exp Eye Res 2002, 74:553–559
76. Grant MB, Caballero S: Somatostatin analogues as drug therapies for retinopathies. Drugs Today (Barc) 2002, 38:783–791
77. Ambler GR, Butler AA, Padmanabhan J, Breier BH, Gluckman PD: The effects of octreotide on GH receptor and IGF-I expression in the GH-deficient rat. J Endocrinol 1996, 149:223–231
78. Gargiulo P, Giusti C, Pietrobono D, La Torre D, Diacono D, Tamburrano G: Diabetes mellitus and retinopathy. Dig Liver Dis 2004, 36(Suppl 1):S101–S105
79. Lahlou H, Guillermet J, Hortala M, Vernejoul F, Pyronnet S, Bousquet C, Susini C: Molecular signaling of somatostatin receptors. Ann NY Acad Sci 2004, 1014:121–131
80. Zhao B, Zhao H, Zhao N, Zhu XG: Cholangiocarcinoma cells express somatostatin receptor subtype 2 and respond to octreotide treatment. J Hepatobiliary Pancreat Surg 2002, 9:497–502
81. Mottet D, Ruys SP, Demazy C, Raes M, Michiels C: Role for casein kinase 2 in the regulation of HIF-1 activity. Int J Cancer 2005, 117: 764–774